Geomechanics and Engineering, *Vol. 29, No. 3 (2022) 219-228*
https://doi.org/10.12989/gae.2022.29.3.219

Machine learning-based regression analysis for estimating Cerchar abrasivity index

No-Sang Kwak[1a] and Tae Young Ko*[2]

[1]*SK C&C Data Platform Group, Seongnam 13558, Republic of Korea*
[2]*Department of Energy and Resources Engineering, Kangwon National University, Chuncheon 24341, Republic of Korea*

(Received December 5, 2021, Revised February 25, 2022, Accepted March 9, 2022)

Abstract. The most widely used parameter to represent rock abrasiveness is the Cerchar abrasivity index (CAI). The CAI value can be applied to predict wear in TBM cutters. It has been extensively demonstrated that the CAI is affected significantly by cementation degree, strength, and amount of abrasive minerals, i.e., the quartz content or equivalent quartz content in rocks. The relationship between the properties of rocks and the CAI is investigated in this study. A database comprising 223 observations that includes rock types, uniaxial compressive strengths, Brazilian tensile strengths, equivalent quartz contents, quartz contents, brittleness indices, and CAIs is constructed. A linear model is developed by selecting independent variables while considering multicollinearity after performing multiple regression analyses. Machine learning-based regression methods including support vector regression, regression tree regression, k-nearest neighbors regression, random forest regression, and artificial neural network regression are used in addition to multiple linear regression. The results of the random forest regression model show that it yields the best prediction performance.

Keywords: Cerchar abrasivity index (CAI); machine learning; regression; rock abrasiveness; wear

1. Introduction

The most widely used parameter to represent rock abrasiveness is the Cerchar abrasivity index (CAI). The Cerchar abrasivity test is a fast and cost-effective method for evaluating rocks abrasiveness (Ko *et al*. 2016). The CAI value can be applied to predict wear in disc cutters used for TBM tunneling. Wear significantly affects the cost and performance of mechanized tunnelling in hard rocks (Saeidi *et al*. 2015, Chang *et al*. 2017). In the CSM model (Rostami 1997), disc cutter life is estimated using the CAI. Disc cutter life, measured in linear meters of rolling on the tunnel face, has been shown to be inversely proportional to the CAI. Gehring (1995) developed a model based on data from several projects to determine the relationship between the CAI and disc cutter wear in milligram steel per meter rolled. Frenzel (2011) examined the correlation between the CAI and radial abrasion of 17-inch disc cutters from various rock types such as sedimentary, metamorphic, and igneous rocks. Liu *et al*. (2017) developed correlations between geological parameters, including the CAI, uniaxial compressive strength (UCS), quartz content (QC), and equivalent quartz content (EQC) and 20-inch cutter life based on field data acquired during the construction of a water conveyance tunnel in China using TBM.

The CAI test was developed in the mid-1980s to investigate the abrasiveness of hard rocks. During the test, a rock specimen is tightly clamped, and the surface of the rock specimen is scratched using a steel pin under a load of 70 N on a distance of 10 mm. This procedure is performed on the rock surface for at least five times in both parallel and perpendicular directions using a new or re-sharpened steel pin. Subsequently, the CAI is determined using the diameter of the worn flat surface (measured in tenths of millimeters) on the test steel pin.

The CAI has been the subject of numerous studies. The effect of geomechanical parameters such as density, porosity, elastic modulus, rock brittleness and strength, as well as those of petrographic factors such as QC and EQC, on CAI were primarily investigated. It was demonstrated extensively that the CAI was significantly affected by the cementation degree, strength, and amount of abrasive minerals, i.e., QC or EQC in the rocks (Al-Ameen and Waller 1994, Plinninger *et al*. 2003, Rostami *et al*. 2014, Ko *et al.* 2016, Moradizadeh *et al*. 2016, Yaralı 2017, Kahraman *et al*. 2018, Ozdogan *et al*. 2018, Erarslan 2019).

According to findings from early investigations, a single factor such as QC and/or rock strength is the most important influencing factor for the CAI (West 1989, Al-Ameen and Waller 1994, Plinninger *et al*. 2003). Recent investigations show that a single parameter is insufficient to explain the factors affecting the CAI (Altindag *et al*. 2010, Ko *et al*. 2016).

In this study, the relationship between rock properties and the CAI was investigated. In particular, the properties of rocks investigated in this study were strength, brittleness, and QC or EQC, which can be measured relatively easily. An extensive database containing information regarding rock types (RTs), uniaxial compressive strengths (UCSs), Brazilian tensile strengths (BTSs), EQCs, QCs, brittleness indexes, and CAIs has been developed.

*Corresponding author, Assistant Professor
E-mail: tyko@kangwon.ac.kr
[a]Ph.D. Tech Specialist

ISSN: 2005-307X (Print), 2092-6219 (Online)

Brittle materials break without exhibiting significant deformation when subjected to stress. A universally accepted standard pertaining to the brittleness of rocks has not been established. The followings are the brittleness indexes used in this study, which are expressed as functions of compressive and tensile strengths of rocks (Meng *et al*. 2021).

$$B_1 = \frac{\sigma_c}{\sigma_t} \tag{1}$$

$$B_2 = \frac{\sigma_c - \sigma_t}{\sigma_c + \sigma_t} \tag{2}$$

$$B_3 = \frac{\sigma_c + \sigma_t}{2} \tag{3}$$

$$B_4 = \frac{\sigma_c \sigma_t}{2} \tag{4}$$

$$B_5 = \sqrt{\frac{\sigma_c \sigma_t}{2}} \tag{5}$$

Where, σ_c is uniaxial compressive strength, and σ_t is Brazilian tensile strength.

The data acquired were processed and examined via single and multiple regression analyses including lasso and ridge regression and five different machine learning based regression techniques. The models were evaluated based on the mean squared error (MSE), mean absolute percentage error (MAPE), and coefficient of determination (R^2).

After performing single and multiple regression analyses, a linear model was developed by selecting independent variables while considering multicollinearity. Machine learning-based regression methods including support vector regression (SVR), regression tree regression (RT), and k-nearest neighbors (KNN) regression, random forest (RF) regression, and artificial neural network (ANN) regression were used in addition to multiple linear regression (MLR).

2. Regression analyses

2.1 Data acquisition and preparation

Data were acquired from published articles and the geotechnical data report of various tunneling projects in the world (Tripathy *et al*. 2015, He *et al*. 2016, Ko *et al*. 2016, Moradizadeh *et al*. 2016, Ündül and Er 2017, Burkhardt *et al*. 2018, Majeed and Bakar 2018, Ozdogan *et al*. 2018, Ansari *et al*. 2020, Kong *et al*. 2021). The data included CAIs, RTs, strength pertaining to the UCS and BTS, petrographic factors of QC and EQC, and brittleness indexes of B_1 to B_5. In addition, a new brittleness index, B_i, which is a function of the UCS and BTS, was proposed based on a nonlinear regression involving the CAI.

$$B_i = \sigma_c^{1/12} \cdot \sigma_t^{1/3} \tag{6}$$

The new brittleness index B_i is expressed as shown in Eq. (6), and the power of the UCS and BTS that maximize R^2 was determined through the method of linear regression analysis by taking the logarithm of both sides assuming the CAI as a power function of the UCS and BTS.

The data included 223 observation data points. Those data points were classified into two groups: training and test sets, which comprised 80% and 20% of the data, respectively.

A histogram of the variables is presented in Fig. 1. The CAI is a dependent feature, and the remaining are independent features.

2.2 Single regression analysis

A single regression was performed based on using the rock types, strength related factors, petrographic factors, and brittleness indexes as independent features, and the CAI as dependent features. The relationships between the CAI and each of the UCS, BTS, QC, EQC, and brittleness indexes B_1 to B_i are depicted in Fig. 2. The BTS, B_5, and B_i were discovered to be correlated with the CAI. However, R^2 was extremely low to be considered statistically significant. Hence, it is concluded that a single feature is inadequate for estimating the value of the CAI.

2.3 Multiple regression analysis

The CAI is a dependent variable, and the other features are independent variables in the multiple regressions. The multiple regressions were conducted using both linear and non-linear models.

MLR analysis was performed to explain the relationship between a dependent variable and two or more independent variables. In the analysis, a model with coefficients is constructed to minimize the residual sum of squares between the observed targets in the dataset and the targets predicted by linear approximation. The linear equation can be expressed as

$$Y = A + B_1 X_1 + B_2 X_2 + \cdots \tag{7}$$

Furthermore, the following non-linear equation is used in the multiple non-linear regression (MNLR) model

$$Y = A \cdot X_1^{B_1} \cdot X_2^{B_2} + \cdots \tag{8}$$

Brittleness indices B_1 through B_i were derived using the UCS and BTS; therefore, the multicollinearity of independent features should be evaluated. Multicollinearity occurs when independent variables in a regression model are correlated. This correlation is problematic because independent variables should be independent. When fitting the model and interpreting the results, a high correlation degree between variables can result in issues. Multicollinearity can be identified based on the variable inflation factor (VIF).

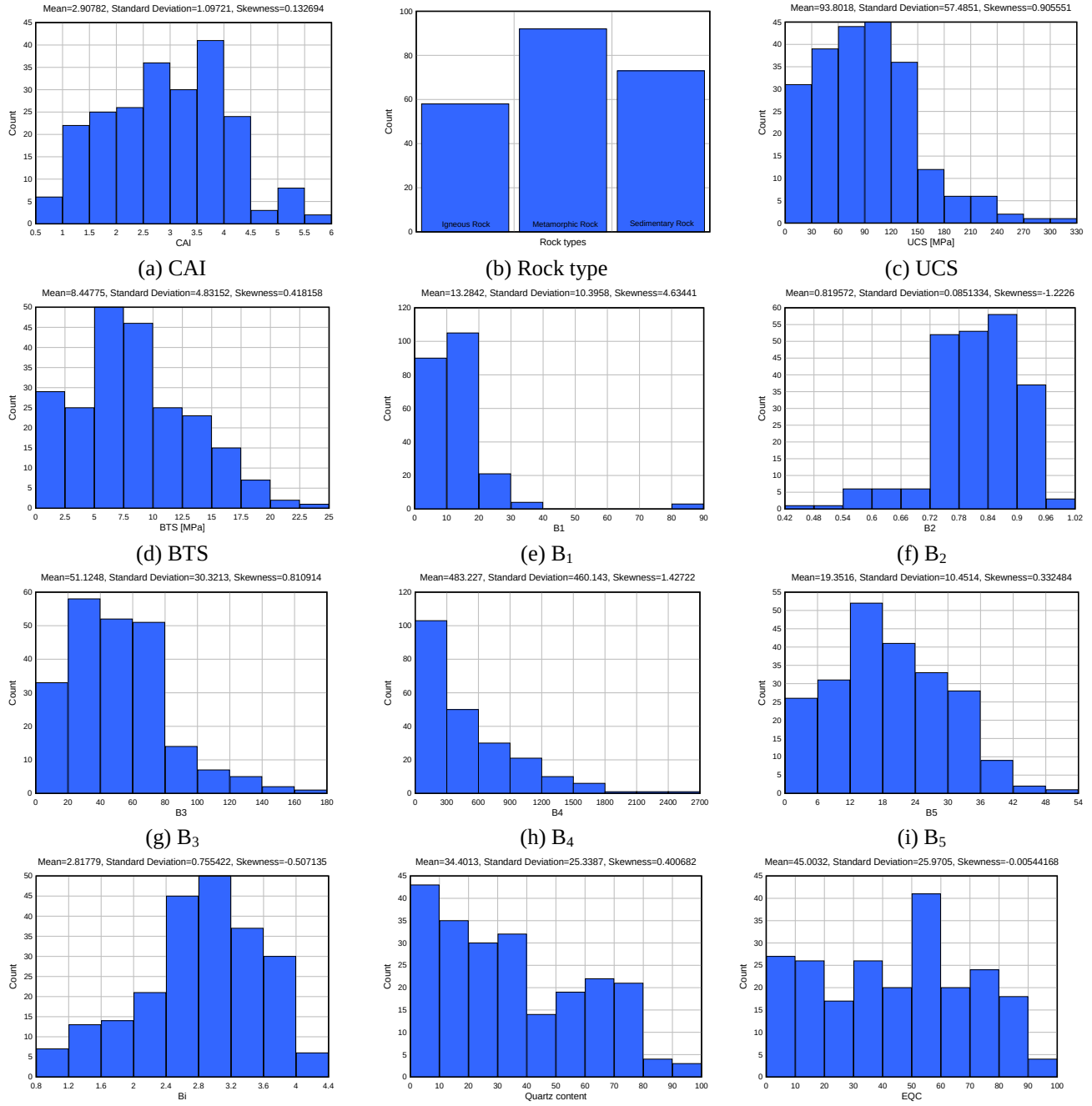

Fig. 1 Histogram of variables

The VIF score of an independent variable represents the level by which the variable is explained accurately using other independent variables. In general, a VIF score exceeding 10 indicates high multicollinearity between the independent variable and the other variables.

In this study, the VIF was calculated for 11 independent variables such as rock types, UCS, BTS, QC, EQC, B_1, B_2, B_3, B_4, B_5, and B_i, and the results are shown in Table 1. Except for rock type and B_1, all other independent variables indicated VIF values exceeding 10, suggesting the occurrence of multicollinearity.

Forward, backward, and stepwise methods were possible for variable selection methods. Stepwise method is a modification of the forward selection so that after each step in which a variable was added, all candidate variables in the model are checked to see if their significance has been reduced below the specified tolerance level. In this study, stepwise method was selected since it yields a simple model that is easy to interpret.

To select a set of variables with sufficient low multicollinearity, a stepwise selection method was performed to remove variables that would result in precision loss when estimating parameters; in particular, the selection was performed beginning with the variable that exhibited the largest VIF (Craney and Surles 2002).

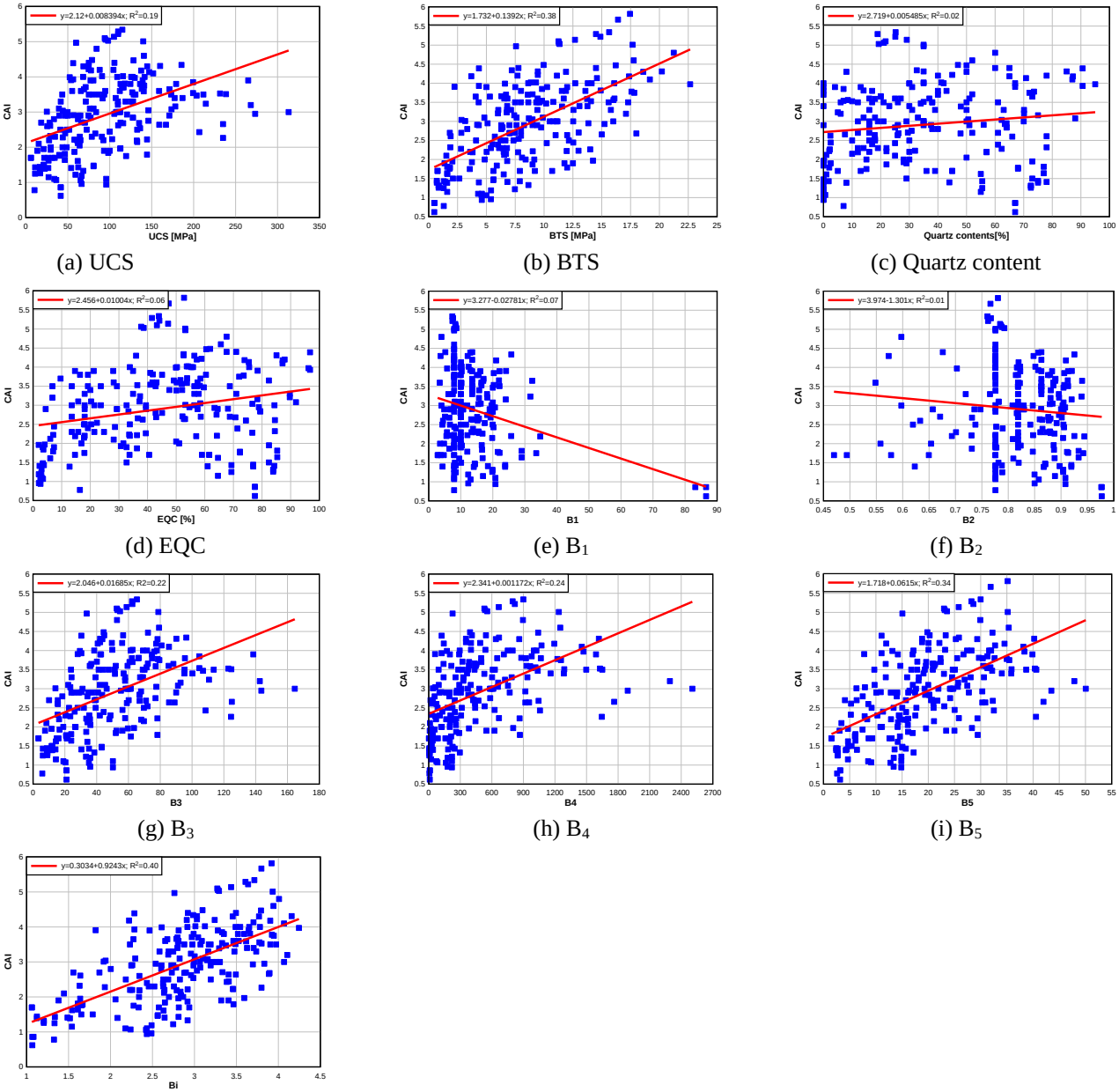

Fig. 2 Relationships between CAI and other factors

Table 1 VIFs for 11 independent variables

	Rock types	UCS	BTS	B_1	B_2	B_3	B_4	B_5	B_i	QC	EQC
VIF	1.82	140.48	180.67	3.59	13.70	89.71	97.97	1151.41	180.38	13.04	12.38

The VIF values for the full set of explanatory variables were computed, after which the variable with the highest VIF was removed. Next, the VIF values were computed again for the reduced set of variables. This is repeated until the largest VIF value was lower than a user defined maximum VIF threshold value.

In the stepwise selection method, rock type, UCS, B_2, B_i, and QC were selected as independent variables, and the calculated VIF values are shown in Table 2.

The best model for predicting the CAI of the MLR based on rock types (RTs), UCS, B_2, B_i, and QC is expressed as follows

$$CAI = 0.017QC - 0.016UCS + 1.839B_i + 6.929B_2 - 0.836RTs - 5.342 \quad (9)$$

where, QC is the quartz contents in %, UCS is the uniaxial compressive strength in MPa, and RTs = 1 for igneous rocks, 2 for metamorphic rocks, and 3 for sedimentary rocks.

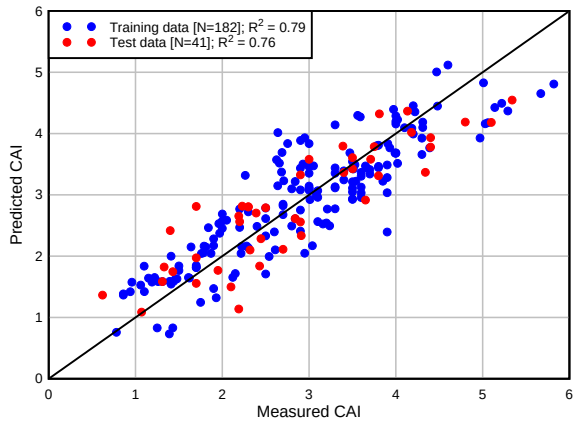

(a) Multiple linear regression

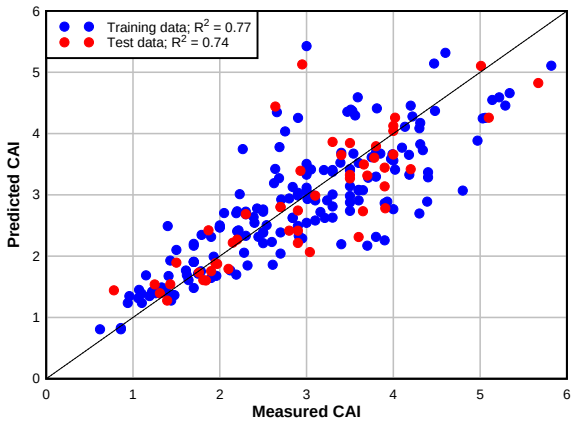

(b) Multiple non-linear regression

Fig. 3 Multiple regression plot

Table 2 VIFs for selected independent variables

	Rock type	UCS	B_2	B_i	QC
VIF	1.233	7.837	3.469	7.197	1.102

The MLR model based on training and test data yielded an R2 of 0.79 and 0.76, respectively.

The best model for predicting the CAI of the MNLR based on rock type, UCS, B_2, B_i, and QC is expressed as follows

$$CAI = 5.432QC^{0.099}UCS^{-0.533}B_2^{2.323}B_i^{2.052}RTs^{-0.382} \quad (10)$$

In the case of nonlinear regression analysis using Eq. (8), when the value of the independent variable is 0, the value of the dependent variable becomes 0 as well. The value of 0 for certain data, such as QC, was replaced with a lower number of 0.1.

The MNLR model based on training and test data yielded an R2 of 0.77 and 0.74, respectively. Fig. 3 shows the regression plot for the training and test data of the multiple linear and non-linear regression model.

2.4 Lasso and Ridge regression analyses

Lasso and Ridge regression are simple techniques to reduce model complexity and prevent over-fitting, which may result from simple linear regressions.

Lasso regression performs L1 regularization, which adds a penalty equal to the absolute value of the magnitude of coefficients. Lasso regression is a type of linear regression that uses shrinkage, which refers to the reduction in data values toward a central value. This particular type of regression is suitable for models that demonstrate high levels of multicollinearity or when automating certain aspects of model selection, such as variable selection/parameter elimination. Ridge regression is a technique for analyzing multiple regression data that reduces the standard errors by adding a degree of bias to the regression estimates (i.e., linear least squares with L2 regularization). Fig. 4 illustrates the results of Lasso and Ridge regression analyses.

Table 3 Evaluation of regression analyses by model

Model	Training data			Test data		
	MSE	MAPE	r^2	MSE	MAPE	r^2
MLR	0.25	17.11	0.79	0.30	16.30	0.77
MNLR	0.40	17.09	0.77	0.38	15.67	0.74
Lasso	0.25	17.01	0.79	0.29	16.03	0.76
Ridge	0.30	18.69	0.76	0.28	14.57	0.76

The model performance was evaluated based on the MSE, MAPE, and R^2. The MSE is typically used as a metric to determine the performance of models, and it is calculated as follows: the MSE is as follows

$$MSE = \frac{1}{n}\sum_{i=1}^{n}(y_i - \overline{y}_i)^2 \quad (11)$$

where, n is the total amount of data, whereas y_i and $\overline{y}_i$ are the observed and predicted values of the variable, respectively. The MSE is the average of the square of difference between the observed and predicted values of a variable.

The MAPE is a measure of prediction accuracy of a forecasting method. It typically expresses accuracy as a ratio, as follows

$$MAPE = \frac{100\%}{n}\sum_{i=1}^{n}\left|\frac{y_i - \overline{y}_i}{y_i}\right| \quad (12)$$

Table 3 shows the evaluation of MLR, MNLR, Lasso, and Ridge regression analyses.

3. Machine learning-based regression analyses

In this study, five different machine learning-based regression methods were employed to predict the CAI. The methods included support vector regression (SVR),

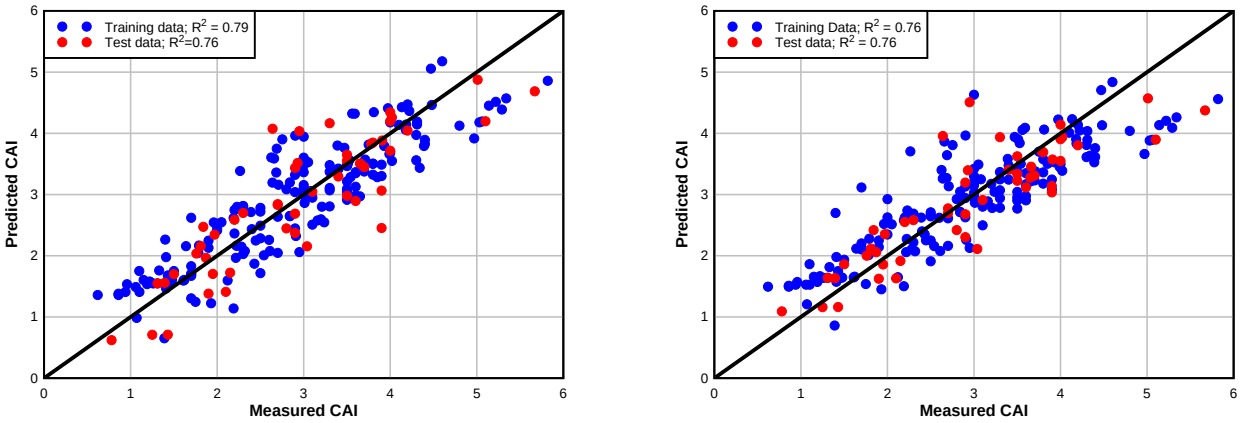

(a) Lasso regression (b) Ridge regression

Fig. 4 Lasso and Ridge regression plot

regression tree (RT), k-nearest neighbors (KNN) regression, random forest (RF) regression, and artificial neural network (ANN) regression. In machine learning-based regression, five independent variables that were used for multiple linear regression, i.e., RTs, UCS, B_2, B_i, and QC were used.

3.1 Support vector regression

SVR is an extension of the support vector machine algorithm. SVR produces models that are only dependent on a portion of the training data, as the cost function used to construct the model ignores any training data that is close to the model prediction. SVR trains using a loss function that penalizes both high and low misestimates equally. The absolute values of errors less than a specific threshold are discarded both above and below the estimate in a symmetrical flexible tube of the minimal radius. Hence, outside the tube, points are penalized; however, points within the tube, either above or below the function, are not penalized. One of the primary benefits of SVR is that its computational complexity is independent of the dimensionality of the input space. It also has a strong generalization capability and a good prediction accuracy. (Drucker *et al*. 1997).

3.2 Regression tree

An RT is a variant of decision trees that is designed to estimate real-valued functions. An RT is built via a process known as binary recursive partitioning, which is an iterative process that segregates the data into partitions or branches, and then continues segregating each partition into smaller groups when ascending each branch.

Initially, all records in the training set are categorized into the same partition. Subsequently, the algorithm begins dividing the data into the first two partitions or branches employing every possible binary split on every field. The algorithm chooses the split that minimizes the sum of the squared deviations from the mean in the two separate partitions. After that, this splitting rule is used on each of the new branches. This process is repeated until each node meets the minimum node size chosen by the user and becomes a terminal node.

3.3 K-nearest neighbors regression

The KNN algorithm uses “feature similarity” to predict values of any new data points. This implies that the new point is assigned a value based on the degree by which it resembles the points in the training set. When implementing regression, the average value is regarded as the final predicted value.

The KNN method is conceptually simple and intuitive, and it can yield the decision boundary in the entire space based on any given training set.

3.4 Random forest regression

An RF is an ensemble technique that can perform both regression and classification tasks using of multiple decision trees and a technique known as “bootstrap and aggregation”, which is typically known as bagging. In this method, the basic idea is to combine multiple decision trees to determine the final output, instead of relying on individual decision trees.

The training data for each decision tree is sampled with replacement from all observations that were originally in the training data set.

Furthermore, the predictor variables considered for splitting any given decision tree are randomly selected from all available predictor variables. Therefore, each decision tree is created on a sample of predictor variables and from a sample of the observations. Repeating this process many times leads to greater diversity in the trees. The final model is a combination of the individual decision trees where the predicted values are averaged.

3.5 Artificial neural networks regression

An ANN is a deep learning algorithm that simulate mechanisms of neurons in the human brain. An ANN comprises an input layer, hidden layers, and an output layer. More than one hidden layer can exist in an ANN. Each layer comprises n neurons. Each layer contains an activation function associated with each of the neurons. The activation function is a function that introduces non-linearity to the

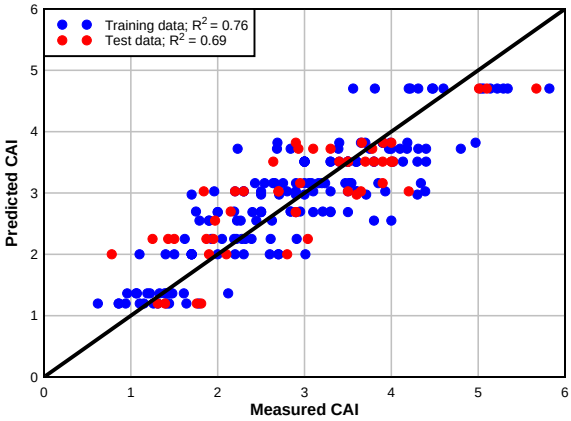

(a) RT regression

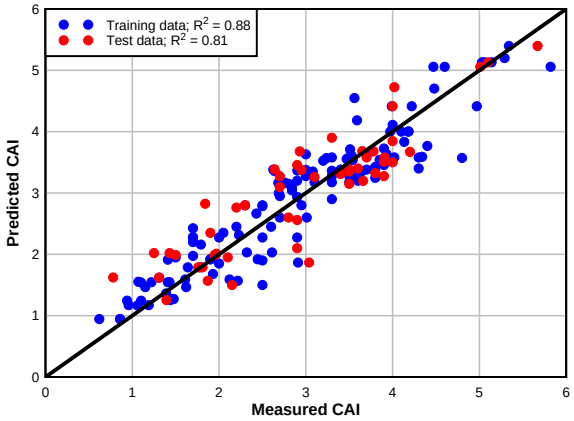

(b) KNN regression

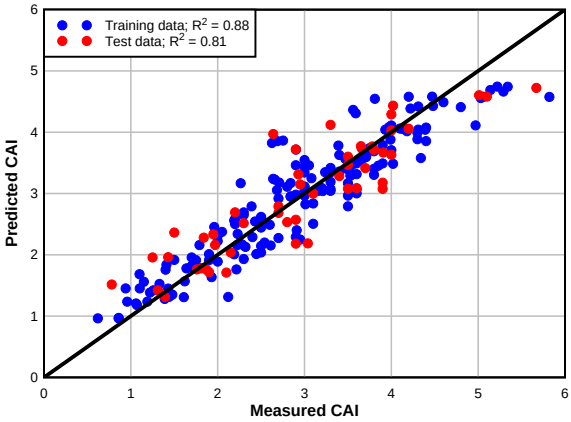

(c) SVM regression

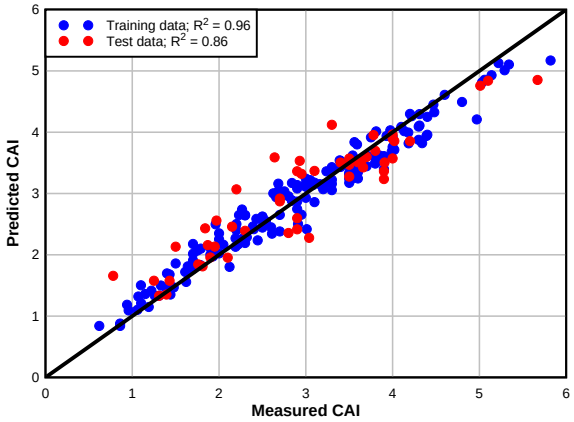

(d) RF regression

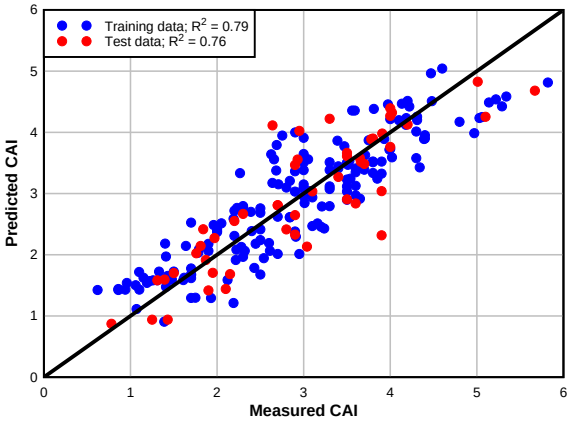

(e) ANN regression

Fig. 5 Machine learning-based regression plot

relationship. An ANN is so flexible that many structures can be constructed to accommodate various types of real-world data. Under the support of today's powerful computing resources, large-scale neural networks can be reliably learned from a huge amount of training data to yield excellent performance for many real-world tasks. At present, neural networks have become the dominant machine learning models for supervised learning.

Table 4 shows the evaluation of models based on machine learning-based regression analyses. Fig. 5 shows the machine learning-based regression plots for both the training and test sets.

Table 4 Model evaluation based on machine learning-based regression analysis

Model	Training data			Test data		
	MSE	MAPE	r^2	MSE	MAPE	r^2
RT	0.30	16.85	0.76	0.35	21.88	0.69
KNN	0.16	12.97	0.88	0.23	16.99	0.81
SVM	0.15	11.81	0.88	0.23	15.02	0.81
RF	0.06	7.39	0.96	0.18	13.65	0.86
ANN	0.06	7.39	0.79	0.18	13.65	0.76

4. Discussion

4.1 Single regression

The distribution of the variables is shown in Fig. 1. The distribution of the CAI, RTs, BTS, B_2, B_5, B_i, and EQC can be approximated using a normal distribution. The distribution of the UCS, B_1, and B_3 is closed to lognormal distribution. The distribution of B_4, and QC shows negative exponential distribution. As discussed in Section 2.2, the relationships between the CAI and each of the UCS, BTS, QC, EQC, and brittleness indexes B_1 to B_i are depicted in Fig. 2. The BTS, B_5, and B_i were discovered to be correlated with the CAI. However, R^2 was extremely low to be considered statistically significant. As such, it is concluded that a single feature is inadequate for estimating the CAI. In fact, this finding has been reported in several publications (Rostami *et al*. 2014, Ko *et al*. 2016, Moradizadeh *et al*. 2016).

4.2 Multiple regression

When all 11 independent variables were used, the R^2 of the multiple linear regression analysis was 0.81. When multiple linear regression analysis was performed using five independent variables that did not cause multicollinearity problems via the stepwise selection method, the R^2 value was 0.79. Among the five independent variables, B_2 and B_i were correlated with brittleness; therefore, a regression analysis was performed using either only B_2 or B_i.

When multiple linear regression analysis was performed by applying four independent variables of QC, UCS, B_i, and RTs, the R^2 was 0.69. Meanwhile, when multiple linear regression analysis was performed using the same independent variables except B_2, which was preplaced with B_i, the R^2 was 0.52.

When reducing from five to four independent variables, the decrease in R^2 was significantly greater as compared with that when reducing from 11 to 5 independent variables. Hence, it is considered appropriate to perform multiple linear regression analysis using five independent variables.

Lasso regression model gives the best results for the multiple regression. The R^2 of Lasso regression was 0.79, which was the highest in the multiple regression models. Also, MSE and MAPE were 0.25 and 17.01, respectively, which were the lowest in the multiple regression models. By contrast, the ridge regression model yielded the worst results for the multiple regression.

Fig. 6 shows the relative importance of the five independent variables. Among the independent variables, Brittleness B_i and rock types were more important, whereas brittleness B_2 was the least important. Because cementation between minerals differs based on the rock types, it is assumed that the rock type significantly affects the CAI.

4.3 Machine learning based regression

The result indicates that the best model was RF regression for the machine learning-based regression. The R^2 of RF regression was 0.96, which was the highest in the machine learning-based regression models. Also, MSE and MAPE were 0.06 and 7.39, respectively, which were the lowest in the machine learning-based regression models.

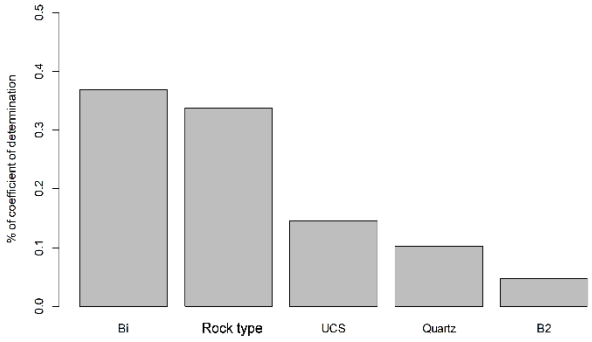

Fig. 6 Relative importance of independent variables

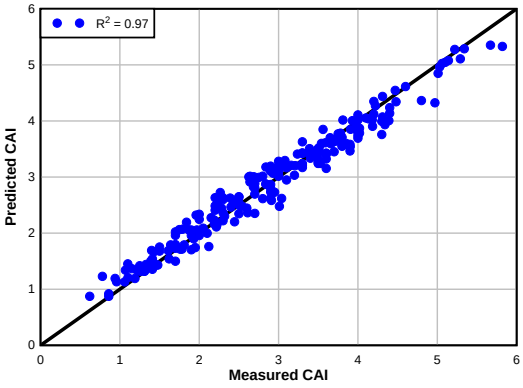

Fig. 7 Overall result for RF regression model

In general, RF regression model yielded the best prediction performance when both the multiple and machine learning-based regressions were considered. Fig. 7 shows the plot of overall result for RF regression model.

4.3 Applications

The CAI can be used to predict the disc cutters consumption in TBM tunneling. Disc cutter life, measured in linear meters of rolling on the tunnel face, has been shown to be inversely proportional to the value of the CAI. Disc cutter life is expressed as follows (Rostami *et al.* 2005)

$$CL = \frac{2057}{CAI} \cdot \frac{D_c}{432} \tag{13}$$

where, CL = linear distance of disc cutter travel on the face in km, D_c = disc cutter diameter in mm.

The wear of cutting tools, including disc cutters, can be measured using a wear coefficient. The wear coefficient (wc) is defined as the ratio of the radial abrasion of the disc cutter ring (a), in mm, to the travelled distance of the disc cutter ring (r), in km, as follows

$$wc[mm/km] = \frac{a[mm]}{r[km]} \tag{14}$$

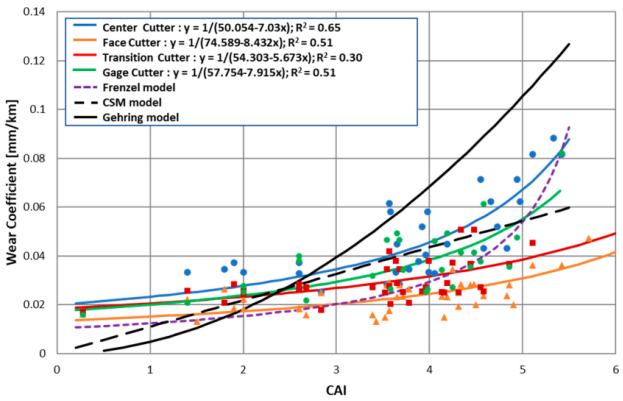

Fig. 8 Relationship between the CAI values and the wear coefficient (Ko and Lee 2020)

Ko and Lee (2020) examined relationship between the CAI and the wear coefficient and Fig. 8 shows the relationship between the CAI and the wear coefficient of 19-inch disc cutters with respect to the cutter position.

5. Conclusions

The purpose of this study was to examine the relationship between rock properties and the CAI. The properties of rocks used in this study were strength, brittleness, and QC or EQC, all of which can be obtained relatively easily. A database comprising 223 observation data points was constructed, which included rock types, UCSs, BTSs, EQCs, QCs, brittleness indices, and CAIs. A linear model was developed by selecting independent variables while considering multicollinearity after performing multiple regression analyses. Machine learning-based regression methods including SVR, RT regression, KNN regression, RF regression, and ANN regression were used in addition to multiple regression. Based on the results, the RF regression model yielded the best prediction performance.

Acknowledgments

This study was supported by 2020 Research Grant from Kangwon National University.

References

Al-Ameen, S.I., and Waller, M.D. (1994), "The influence of rock strength and abrasive mineral content on the Cerchar Abrasive Index", *Eng. Geol.*, **36**(3-4), 293-301. https://doi.org/10.1016/0013-7952(94)90010-8.

Altindag, R., Sengun, N., Sarac, S., Mutluturk, M. and Guney, A. (2010), "Evaluating the relations between brittleness and Cerchar abrasion index of rocks", *Proceedings of the Regional Symposium of the International Society for Rock Mechanics*, EUROCK 2009, Dubrovnik, Cavtat, Croatia.

Ansari, M., Hosseini, M. and Taleb Beydokhti, A.R. (2020), "A correlation for estimating LCPC abrasivity coefficient using rock properties", *J. Min. Environ.*, **11**(3), 799-808. https://doi.org/10.22044/jme.2020.9520.1863.

Burkhardt, M, Kim, E. and Nelson, P.P. (2018), "EMI database analysis focusing on relationship between density and mechanical properties of sedimentary rocks", *Geomech. Eng.*, **14**(5), 491-498. https://doi.org/10.12989/gae.2018.14.5.491.

Chang, S.H., Lee, C., Kang, T.H., Ha, T. and Choi, S.W. (2017), "Effect of hardfacing on wear reduction of pick cutters under mixed rock conditions", *Geomech. Eng.*, **13**(1), 141-159. https://doi.org/10.12989/gae.2017.13.1.141.

Craney, T.A. and Surles, J.G. (2002), "Model-dependent variance inflation factor cutoff values", *Qual. Eng.*, **14**(3), 391-403. https://doi.org/10.1081/QEN-120001878.

Drucker, H., Burges, C.J., Kaufman, L., Smola, A. and Vapnik, V. (1997), "Support vector regression machine", *Proceedings of the 1996 Conference Advances in Neural Information Processing Systems 9*.

Erarslan, N. (2019), "Assessment of Cerchar abrasivity test in anisotropic rocks", *Geomech. Eng.*, **17**(6), 527-534. https://doi.org/10.12989/gae.2019.17.6.527.

Frenzel, C. (2011), "Disc cutter wear phenomenology and their implications on disc cutter consumption for TBM", Proceedings of the 45th US Rock Mechanics/ Geomechanics Symposium, San Francisco, U.S.A. June.

Gehring, K. (1995), "Leistungs- und Verschleissprognosen im maschinellen", *Tunnelbau Felsbau*, **13**(6), 439-448.

He, J., Li, S., Li, X., Wang, X. and Guo, J. (2016), "Study on the correlations between abrasiveness and mechanical properties of rocks combining with the microstructure characteristic", *Rock Mech. Rock Eng.*, **49**. 2945-2951. https://doi.org/10.1007/s00603-015-0862-3.

Kahraman, S., Fener, M., Käsling, H. and Thuro, K. (2018), "Investigating the effect of strength on the LCPC abrasivity of igneous rocks", *Geomech. Eng.*, **15**(2), 805-810. https://doi.org/10.12989/gae.2018.15.2.805.

Ko, T.Y., Kim, T.K., Son, Y. and Jeon, S. (2016), "Effect of geomechanical properties on Cerchar Abrasivity Index (CAI) and its application to TBM tunnelling", *Tunn. Undergr. Sp. Tech.*, **57**, 99-111. https://doi.org/10.1016/j.tust.2016.02.006.

Ko, T.Y. and Lee, S.S. (2020), "Effect of rock abrasiveness on wear of shield tunnelling in Bukit Timah granite", *Appl. Sci.*, **10**(9), 3231, https://doi.org/10.3390/app10093231.

Kong, F., Xue, Y., Qiu, D., Li, Z., Chen, Q. and Song, Q. (2021), "Impact of grain size or anisotropy on correlations between rock tensile strength and some rock index properties", *Geomech. Eng.*, **27**(2), 131-150. https://doi.org/10.12989/gae.2021.27.2.131.

Liu, Q., Liu, J., Pan, Y., Zhang, X., Peng, X., Gong, Q. and Du, L. (2017), "A wear rule and cutter life prediction model of a 20-in. TBM cutter for granite: A case study of a water conveyance tunnel in China", *Rock Mech. Rock Eng.*, **50**, 1303-1320. https://doi.org/10.1007/s00603-017-1176-4.

Majeed, Y. and Abu Bakar, M.Z. (2018), "A study to correlate LCPC rock abrasivity test results with petrographic and geomechanical rock properties", *Q. J. Eng. Geol.*, **51**(3), 365-378. http://doi.org/10.1144/qjegh2017-112.

Meng, F., Wong, L.N.Y. and Zhou, H. (2021), "Rock brittleness indices and their applications to different fields of rock engineering: A review", *J. Rock Mech. Geotech. Eng.*, **13**, 221-247. https://doi.org/10.1016/j.jrmge.2020.06.008.

Moradizadeh, M., Cheshomi, A., Ghafoori, M. and TrighAzali, S. (2016), "Correlation of equivalent quartz content, Slake durability index and Is50 with Cerchar abrasiveness index for different types of rock", *Int. J. Rock Mech. Min. Sci.*, **86**, 42-47. https://doi.org/10.1016/j.ijrmms.2016.04.003.

Ozdogan, M.V., Deliormanli, A.H. and Yenice, H. (2018), "The correlations between the Cerchar abrasivity index and the

geomechanical properties of building stones", *Arab. J. Geosci*., **11**, 604. https://doi.org/10.1007/s12517-018-3958-8.

Plinninger, R., Kasling, H., Thuro, K. and Spaun, G. (2003), "Testing conditions and geomechanical properties influencing the CERCHAR abrasiveness index (CAI) value", *Int. J. Rock Mech. Min. Sci*., **40**, 259-263. https://doi.org/10.1016/S1365-1609(02)00140-5.

Rostami, J. (1997), "Development of a Force Estimation Model for Rock Fragmentation with Disc Cutters through Theoretical Modeling and Physical Measurement of Crushed Zone Pressure", Ph.D. Thesis, Colorado School of Mines, Golden, Colorado, USA

Rostami, J., Ghasemi, A., Gharahbagh, E.A., Dogruoz, C. and Dahl, F. (2014), "Study of dominant factors affecting Cerchar abrasivity index", *Rock Mech. Rock Eng*., **47**(5), 1905-1919. https://doi.org/10.1007/s00603-013-0487-3.

Rostami, J., Ozdemir, L., Bruland, A. and Daul, F. (2005), "Review of issues related to Cerchar abrasivity testing and their implications on investigations and cutter cost estimates", *Proceedings of the Rapid Excavation and Tunneling Conference (RETC)*, Seattle, U.S.A.

Saeidi, O., Elyasi, A. and Torabi, S.R. (2015), "Wear assessment of the WC/Co cemented carbidetricone drillbits in an open pit mine", *Geomech. Eng*., **8**(4), 477-493. https://doi.org/10.12989/gae.2015.8.4.477.

Tripathy, A., Singh, T.N. and Kundu, J. (2015), "Prediction of abrasiveness index of some Indian rocks using soft computing methods", *Measurement*, **68**, 302-309. https://doi.org/10.1016/j.measurement.2015.03.009

Ündül, Ö. and Er, S. (2017), "Investigating the effects of micro-texture and geo-mechanical properties on the abrasiveness of volcanic rocks", *Eng. Geol*., **229**, 293-301. http://doi.org/10.1016/j.enggeo.2017.09.022.

West, G. (1989), "Rock abrasiveness testing for tunnelling", *Int. J. Rock Mech. Min. Sci. Geomech. Abstr*., **26**(2), 151-160. https://doi.org/10.1016/0148-9062(89)90003-X.

Yaralı, O. (2017), "Investigation into relationships between Cerchar hardness index and some mechanical properties of coal measure rocks", *Geotech. Geol. Eng*., **35**, 1605-1614. https://doi.org/10.1007/s10706-017-0195-y.